JOURNAL OF MATERIALS SCIENCE 30 (1995) 4839–4846

Observations on crystal growth mechanisms in the directionally solidified high temperature superconductor $Y_1Ba_2Cu_3O_{7-\delta}$

E. J. HARDMAN
Department of Materials Science and Engineering, University of Liverpool, Liverpool, L69 3BX, UK

D. G. McCARTNEY*
Department of Materials Engineering and Materials Design, University of Nottingham, University Park, Nottingham NG7 2RD, UK

X. YAO
Division 4, Superconductivity Research Laboratory, International Superconductivity Technology Center, Tokyo, Japan

The growth behaviour of $Y_1Ba_2Cu_3O_{7-\delta}$(Y1-2-3) crystals has been studied by horizontal directional solidification of samples heated into the liquid (L) plus $Y_2Ba_1Cu_1O_5$(Y2-1-1) phase field. Cylindrical samples of initially stoichiometric Y1-2-3 composition were solidified at rates ranging from 1 to 10 mm h^{-1} using temperature gradients between 2.5 and 5 K mm^{-1}. A novel method was employed to support the L + Y2-1-1 semi-solid and minimize reaction with the crucible. Selected samples were quenched during solidification so that growth mechanisms could be studied. Quasi-single crystals of Y1-2-3 formed, providing that the growth rate did not exceed 1 mm h^{-1} and that the temperature gradient was > 3.5 K mm^{-1}. The quasi-single crystals contained particles of Y2-1-1 as well as Ba–Cu-rich bands as secondary phases and had a preferred orientation of [0 0 1] at 45° to the growth axis when grown from a polycrystalline seed crystal. No preferred orientation developed when samples were grown without a seed. In quenched samples, macroscopic growth steps were observed on the (0 0 1) plane, and within the cylindrical sample the faces of the growing crystal were found to be mutually perpendicular planes. During solidification liquid was found to be lost from the L + Y2-1-1 semi-solid region of the sample. This occurred both by wetting of the support bars and by liquid migration into the seed crystal region.

1. Introduction

It has now been widely demonstrated that (at 77 K) critical current densities, J_c, of the order of 10^5 A cm^{-2} in zero field are achievable in bulk, high-temperature superconductors based on $Y_1Ba_2Cu_3O_{7-\delta}$(Y1-2-3) which have been partially melted and then resolidified to give a textured (or aligned) grain structure (Refs 1 and 2 provide good reviews of the topic). Furthermore, such materials are found to have appreciable J_c values even in fields of several Tesla (T). It is the phase transformations occurring during melting and resolidification which can, under proper conditions, produce these aligned (or textured) microstructures. Depending on the experimental conditions, textured domains of the Y1-2-3 phase ranging in length from several hundred micrometres to >20 mm can be produced. The pioneering work in this area was carried out by Jin *et al.* [3, 4] and subsequently several different procedures for producing highly textured regions in samples have been reported in the literature (see for example Refs 1, 2 and 3–9). The term melt-texturing, or melt-textured growth, has thus come to be used to describe a number of related but subtly different experimental procedures. In essence, though, all melt-texturing techniques rely on the fact that the Y1-2-3 phase melts incongruently when heated in air or oxygen. In air the melting temperature is ca. 1010 °C [10, 11] and the incongruent melting reaction is as follows

$$Y_1Ba_2Cu_3O_{7-\delta}(\text{Y1-2-3}) \rightarrow Y_2Ba_1Cu_1O_5(\text{Y2-1-1}) + \text{liquid (L)}$$

The composition of the liquid phase is not known precisely but the ternary phase diagrams of Refs 10 and 11 indicate that it is significantly richer in Ba and Cu than the Y1-2-3 phase. Slow cooling from the partially molten state (just above 1010 °C), using

*Author to whom communication should be addressed.

0022–2461

cooling rates $< 3\ K\ h^{-1}$, is then normally employed to produce large grains or even quasi-single crystals of the Y1-2-3 phase. Many variations on this basic procedure have been reported in the literature as a means of obtaining well textured samples or domains within samples. For example, Salama *et al.* [6] have cooled samples slowly in a very low temperature gradient, whereas McGinn *et al.* [5], Pollard *et al.* [9], Jin *et al.* [2, 3] and others [1, 2], have employed solidification in a steep temperature gradient in an effort to promote directional solidification and alignment of the Y1-2-3 phase with the a–b, i.e. (0 0 1), planes of the crystal structure parallel to the heat flow direction for optimum superconducting properties. Murakami *et al.* [8] have adopted additional heating and cooling stages in order to control the size distribution of the Y2-1-1 phase prior to slow cooling through the peritectic temperature.

Despite the widespread interest in melt-textured growth as a technique for producing high J_c, high transition temperature (T_c) superconductors there remains a somewhat limited understanding of the mechanisms of crystal growth in the stoichiometric Y1-2-3 system. Furthermore, a number of important questions relating to this do not appear to have been adequately addressed. For example, on slow cooling through the peritectic temperature the Y2-1-1 phase does not seem to nucleate the Y1-2-3 phase. This behaviour is rarely observed in common metallurgical alloy systems [12]. In addition, the Y1-2-3 phase solidifies as a faceted crystal, enveloping the pre-existing Y2-1-1 phase as it grows. It develops a three-dimensional crystal (or grain) shape significantly different from that of Y1-2-3 crystals grown directly from single-phase Ba–Cu-rich melts; these melt-flux grown crystals often form as thin single crystal platelets [13–15].

The main purpose of this paper is to clearly describe experimental procedures which have been used to obtain melt-textured, quasi-single crystal samples, and to highlight important observations on fundamental aspects of the crystal growth process.

Samples which have been prepared by the melt-texturing route described herein become superconducting with a transition temperature of ca. 90 K after annealing in pure oxygen at temperatures $< 600\ °C$. However, it is not the purpose of this paper to present results on magnetic or electrical properties as these have already been published elsewhere [16, 17].

2. Experimental procedure

Rods of Y1-2-3, 1 or 2 mm in diameter and 40–80 mm in length, formed the starting material for all the experiments reported in this paper. All rods were of stoichiometric $Y_1Ba_2Cu_3O_{7-\delta}$ composition and had a sintered, polycrystalline, single-phase grain structure. The average grain size was $< 10\ \mu m$ and the volume fraction of porosity was typically between 0.05 and 0.15. These rods were supplied by ICI Advanced Materials, Runcorn, UK, and had been manufactured using a proprietary plastic extrusion process [18]. All melting and resolidification experiments were carried out in horizontal tube furnaces in air. The inner furnace tube and sample boat were made from high purity recrystallized alumina. In order to minimize the reaction between alumina and the Ba–Cu-rich melt which forms above 1010 °C the Y1-2-3 sample was not allowed to rest directly on the sample boat. Instead it was supported, at intervals of ca. 10 mm, by small diameter recrystallized alumina tubes placed transversely underneath it (dimensions of the tubes were 0.5 mm outer diameter and 0.2 mm inner diameter). Fig. 1 shows a macrophotograph of a solidified rod prior to its removal from such supports.

In the experiments reported in this paper undirectional solidification was performed by pulling the alumina boat, which carried the supported rod (initially of stoichiometric Y1-2-3 composition) from the hot zone of a tube furnace. Pulling rates, ranging from 1 to 5 $mm\ h^{-1}$, were investigated and several different hot-zone configurations were employed to enable the furnace temperature gradients to be varied. Normally two separate sets of furnace windings were used to give the desired furnace profile and temperature stability. As crystal growth occurs below the equilibrium melting temperature, the furnace temperature gradients quoted in this work were measured at 980 °C. A number of samples were grown using gradients in the range of 2.5 to 5 $K\ mm^{-1}$, and they were normally pulled for times ranging from 24 to 48 h, depending on the lengths of grown crystal required. After pulling ceased the solidified rods were cooled to room temperature under furnace cooling conditions (i.e. ca. 50 $K\ h^{-1}$), except for those which were quenched during growth in order to "freeze-in" and retain the shape of the crystal-growth front. A rapid quench, sufficient to preserve the as-growing morphology, was achieved by rapidly pulling the rod from the furnace and allowing it to cool in air at room temperature.

The furnaces were controlled by self-tuning controllers, and furnace stability was checked by placing a Pt–Pt/13% Rh thermocouple, of wire diameter 0.3 mm, at various locations along the furnace tube axis. Long- and short-term stability was always better than $\pm$ 0.2 K. The stability of the stepper motor drive system was also checked by monitoring the steady change in temperature of a thermocouple as it was pulled at 1 $mm\ h^{-1}$ from the furnace hot zone whilst

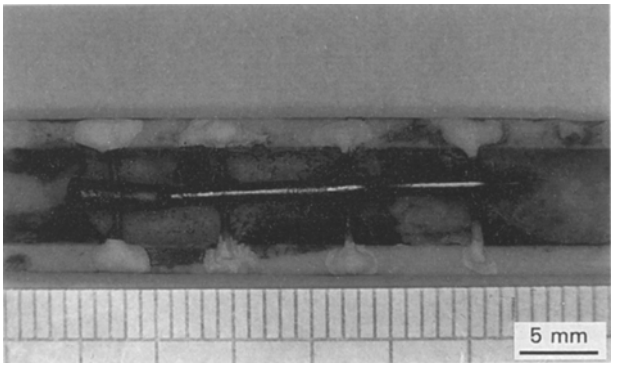

Figure 1 Macrophotograph showing the solidified Y1-2-3 sample supported by thin alumina rods fixed to an alumina boat. The unmelted polycrystalline region is at the left.

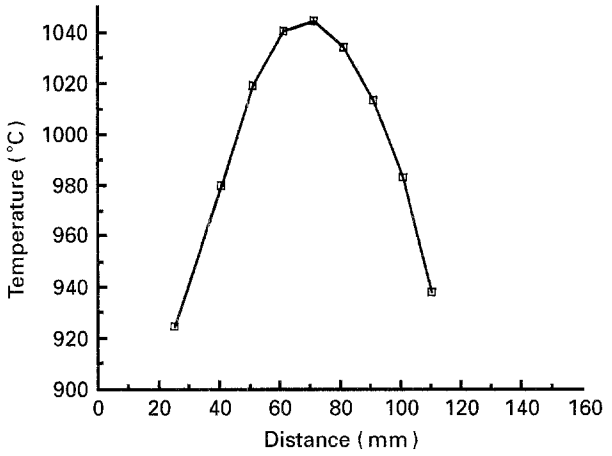

Figure 2 Plot of temperature versus position within the hot zone of the furnace.

fixed to the boat which normally carried the Y1-2-3 sample rod. Mechanical instabilities were found not to occur. Fig. 2 shows a furnace temperature profile typical of those employed in the present work. The Y1-2-3 sample rod was allowed to stabilize for up to 2 h in the hot furnace before pulling was begun. It was normally carefully positioned to ensure that a known length of the polycrystalline material remained unmelted (typically 5 mm) whilst the remainder was heated above the incongruent melting temperature and into the liquid (L) plus Y2-1-1 phase field. The maximum furnace temperature did not exceed 1040 °C.

Samples were prepared for optical microscopy by mounting in cold-setting resin, grinding on SiC paper and polishing with a colloidal silica solution. Alcoholic ferric chloride was found to be a useful etching reagent for revealing the structure at quenched interfaces. Grain structures were generally observed in unetched samples using polarized light optical microscopy. Electron probe microanalysis was used to determine compositions in the quenched regions of samples. Analysis was performed on a Cameca electron microprobe using wavelength dispersive spectrometry for all of the elements.

3. Results

3.1. Effect of thermal processing parameters on microstructural development

At a pulling rate, V, of 1 mm h^{-1} and with temperature gradients in the range of 3.5–5 K mm^{-1}, solidification was invariably initiated by a number of grains of the Y1-2-3 phase growing from the initial polycrystalline solid–liquid interface. As solidification progressed the number of grains decreased until the entire cross-section of the rod was normally occupied by a crystal of single orientation. Fig. 3 is a low magnification longitudinal section of a rod which illustrates the development of this structure. The microstructure within the single crystal grain is shown in Fig. 4 and, as observed previously [19], consists of globules of the Y2-1-1 phase surrounded by a matrix of Y-1-2-3 and layers of a Ba–Cu-rich phase. The Ba–Cu-rich layers are known to be parallel to the (0 0 1), or a–b, plane of

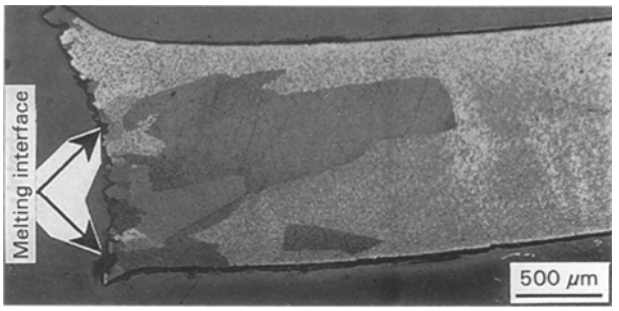

Figure 3 Optical micrograph showing a longitudinal section of the solidified bar in the region of the interface between the unmelted, polycrystalline and partially melted regions. The development of a single grain (at the right) from a number of much smaller grains is illustrated. (Taken using polarized light.)

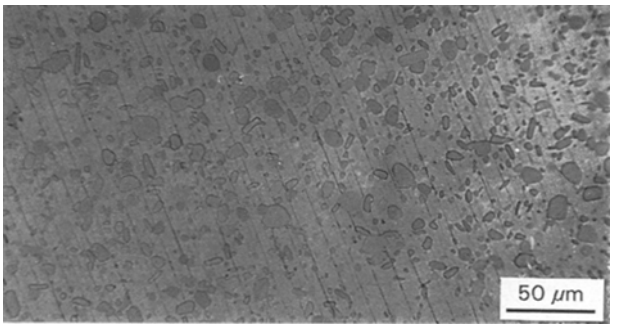

Figure 4 Optical micrograph showing a longitudinal section of a quasi-single crystal region. Globules of the Y2-1-1 phase in a matrix of Y1-2-3 are visible together with the thin Ba–Cu-rich layers. Etched in alcoholic ferric chloride.

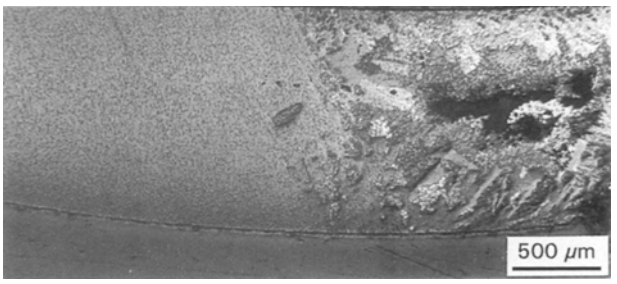

Figure 5 An optical micrograph from a longitudinal section illustrating the breakdown of quasi-single crystal growth. Taken under polarized light with the black areas and white areas both being regions of CuO. The single crystal region is at the left and the polycrystalline region at the right.

the Y1-2-3 crystal structure [9, 19]. With the conditions $V = 1$ mm h^{-1} and $G = 3.5$ K mm^{-1} it was possible to grow the quasi-single crystal for distances of up to 20 mm along the length of the rod. However, its growth was eventually terminated by the formation of a polycrystalline grain structure which included significant amounts of CuO, as shown in Fig. 5. The presence of copper oxide was confirmed using energy dispersive X-ray analysis in a scanning electron microscope.

When the pulling rate was increased to either 2 or 5 mm h^{-1} at the same gradient of 5 K mm^{-1} a polycrystalline grain structure developed with the formation of roughly equiaxed grains of the Y1-2-3 phase

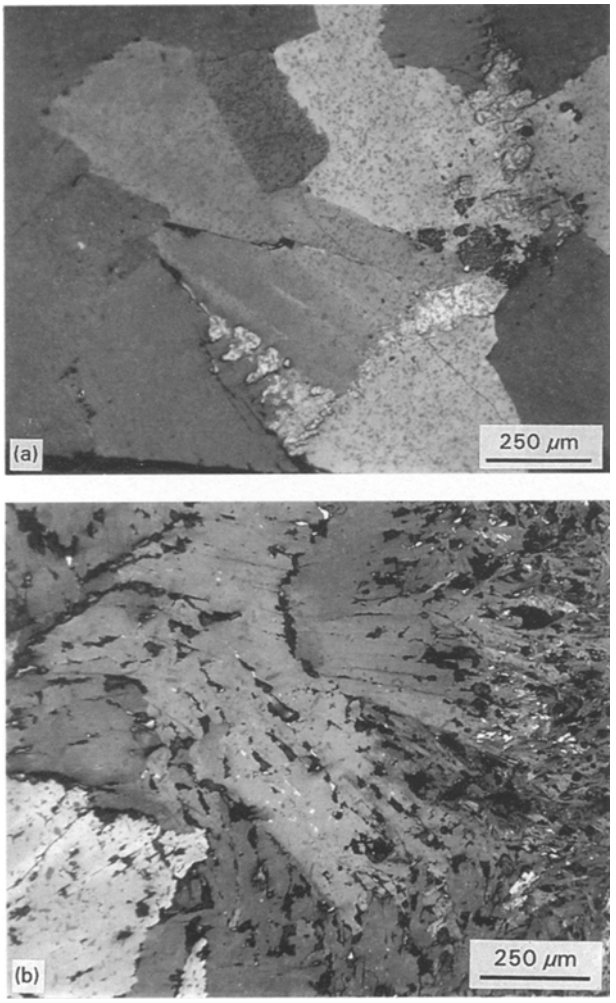

Figure 6 Polarized light optical micrographs showing the equiaxed grain structures which developed at pulling rates (mm h^{-1}) of: (a) 5; and (b) 10.

several hundred micrometres in size. At $V = 10\ mm\ h^{-1}$ the polycrystalline grains developed a fan-shaped morphology; these features are shown in Fig. 6a and b, respectively. On reducing the gradient to 2.5 K mm^{-1} a polycrystalline grain structure, with grains several millimetres in length, developed even at the lowest pulling rate of 1 mm h^{-1}. However, quasi-single crystal growth was not possible.

To summarize, it was found that gradients $> 3.5\ K\ mm^{-1}$ must be employed, at growth rates of no more than 1 mm h^{-1}, if a quasi-single crystal structure is to be achieved.

3.2. Orientation of quasi-single crystals

In six separate samples, each grown from an unmelted polycrystalline seed, the orientation of the dominant quasi-single crystal was determined. Knowing that the Ba–Cu-rich layers in the microstructure are parallel to the (0 0 1) plane of the Y1-2-3 crystal, then orientations can be rapidly determined using two-surface analysis of sectioned crystals [20] in an optical microscope. It was found that the c-axis ([0 0 1] direction) of the dominant Y1-2-3 crystal was at an angle of ca. 45° to the axis of the rod in all samples. It was also found that no such preferred orientation developed when the sample was positioned in the furnace such that an unmelted seed portion was not retained.

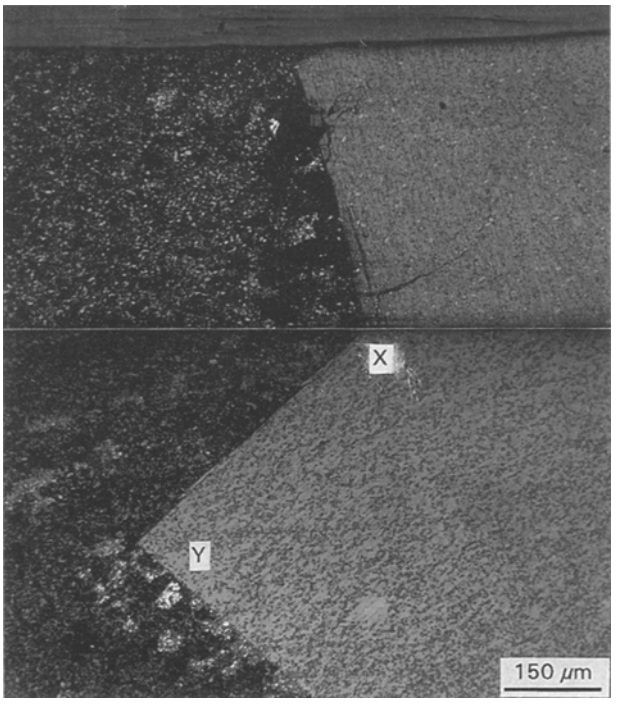

Figure 7 Optical micrograph showing two longitudinal sections (ca. 90° apart) through a quenched interface. The Y1-2-3 matrix, Y2-1-1 globules and Ba–Cu-rich layers are all clearly visible in the crystal which is growing from right to left. Magnified views of regions X and Y are shown in Fig. 9.

3.3. Observations on growth-front morphology

Typically, samples were quenched after 10 mm of a single-crystal orientation had been grown. The quenched interface was examined on two longitudinal planes 90 ° apart; a typical structure is shown in Fig. 7. A faceted morphology is clearly visible with one of the growth planes being parallel to the Ba–Cu-rich layers [i.e. the (0 0 1) plane of Y1-2-3]. A more complete picture of the growth morphology was obtained by taking sequential cross-sections through a quenched sample at known distances from the tip of the growing solid. Fig. 8a shows a sequence of such transverse sections and Fig. 8b a graphical reconstruction of the sequence of positions. Accurate measurements of angles and distances were taken during sectioning and it was found that the faces of the growing crystal were mutually perpendicular. Thus, the growing crystal can be likened to a cube-corner growing within the cylindrical sample.

Quenched interfaces were also examined in the optical microscope at a higher magnification and these revealed the presence of growth steps on the Y1-2-3 interface parallel to the (0 0 1) plane as shown in Fig. 9a. It is also seen from Fig. 9a and b that Y2-1-1 particles are incorporated into the Y1-2-3 at both growing interfaces. In the quenched liquid region particles of Y2-1-1 are difficult to identify using optical microscopy because of difficulties in preparing well-polished samples of this material. However, their

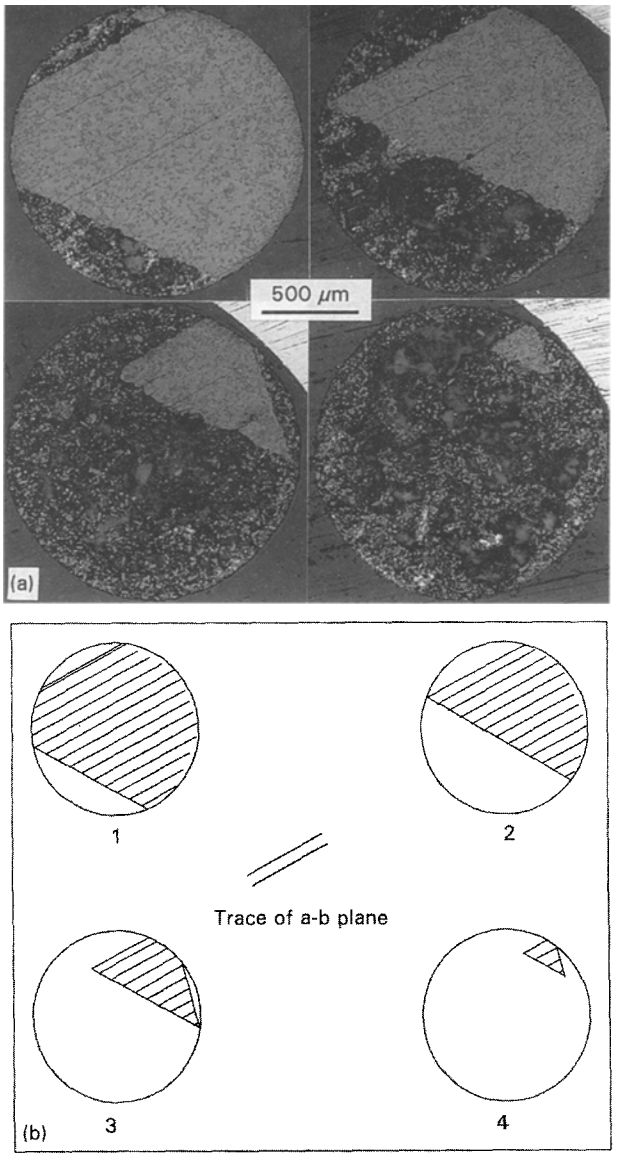

Figure 8 (a) Optical micrographs showing a sequence of transverse sections through a quenched interface. The distance from the tip of the crystal is decreasing from top left to bottom right. (b) Schematic illustration of (a) where 1–4 indicate decreasing distances from the tip.

presence has been confirmed by both electron microprobe microanalysis and transmission electron microscopy [19, 21, 22].

3.4. Growth-front temperature and sample composition

It can be seen from Figs 7 and 8 that the crystal grows over a temperature interval. In order to determine this interval it is necessary to know the temperature gradient in the sample as well as the distance from the tip to the base of the crystal. Assuming the furnace temperature gradient was a reasonable approximation to the gradient in the sample, and taking measurements from samples sectioned sequentially on transverse planes (as in Fig. 8), it was found that crystals were growing over temperature intervals of the order of 3–5 K. The approximate solid–liquid interface growth temperature was also estimated from the known furnace

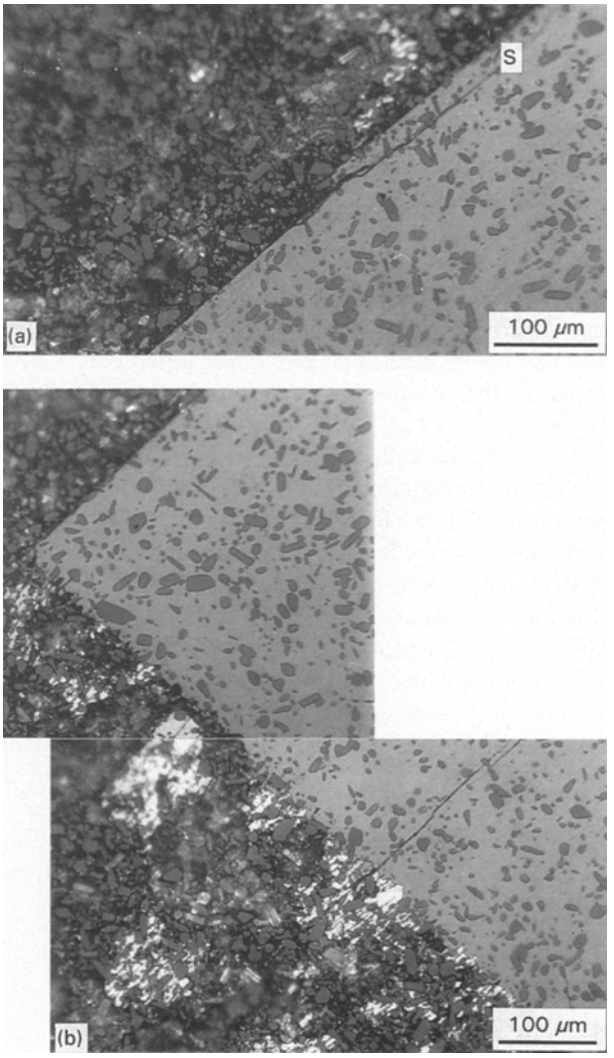

Figure 9 (a) Magnified view of region X of the quenched growth front shown in Fig. 7. A macroscopic growth step is visible at S on the (0 0 1) plane. (b) Magnified view of region Y of the quenched growth front shown in Fig. 7. The interface is perpendicular to the (0 0 1) plane.

temperature profile, and the position of the sample at the time of quenching. Growth temperatures were found to be ca. 940 °C. This can only be regarded as an approximate value but is certainly well below the equilibrium peritectic melting temperature of Y1-2-3, which is 1010 °C in air.

Measurements of the average composition of the quenched region ahead of the growth front were obtained using electron probe microanalysis. A large number of area analyses were performed on regions 40 × 40 μm, and the overall average composition was found to be: 11 at % Y; 11 at % Ba; 24 at % Cu; and 54 at % O. Clearly, the bulk composition of the solidifying sample was significantly different from that of Y1-2-3 (which is ca: 8 at % Y; 17 at % Ba; 25 at % Cu; 50 at % O). In addition to measuring average compositions of the quenched region, spot analyses were performed to determine the composition of the quenched liquid between the Y2-1-1 particles. This liquid was found to have a composition very close to $BaCuO_2$ with an yttrium content in the range of 0.2–0.6 at %.

Thus, the low interface growth temperature of 940 °C must be considered in the light of the overall

composition from which solidification is taking place, as discussed in a subsequent section.

4. Discussion

The results described represent a detailed study of grain structure and microstructure development during directional solidification of $Y_1Ba_2Cu_3O_{7-\delta}$. When analysing the above observations it is crucial to remember that the system possesses several notable characteristics. Firstly, solidification is taking place from a viscous, semi-solid mixture of liquid plus Y2-1-1 in which the volume fraction of the latter is estimated to be ca. 0.35 [22, 23]. Secondly, the oxide melt is highly reactive with virtually all crucible substrates, including recrystallized alumina. Thirdly, liquid can migrate readily when in contact with alumina, which it wets, and so can effectively be lost from the solidifying system. These and other factors mean that it can be difficult to distinguish intrinsic characteristics of the solidification phenomena from features which are artefacts of the experimental procedure or sample preparation methods. Aspects of the results which are considered to reflect intrinsic phenomena are: the growth mechanisms leading to the incorporation of Y2-1-1 into Y1-2-3; the underlying factors which give rise to the preferred crystal orientation, including grain structure development. These will be considered in the following sections, along with the deviation of bulk sample composition from stoichiometry.

4.1. Grain structure development

It is apparent that in directionally solidified samples, grown at $1\,mm\,h^{-1}$ at a gradient of at least $3.5\,K\,mm^{-1}$, a process of grain elimination, i.e. competitive growth, was responsible for the formation of a quasi-single crystal from the original, fine-grained, polycrystalline seed. Fig. 3 illustrates this and the preferred orientation of [0 0 1] at 45° to the growth axis has also been noted by both Cima *et al.* [24] and McGinn *et al.* [5]. This preferred orientation in seeded samples can be contrasted with results obtained from experiments in which a sample was placed in the furnace such that no unmelted Y1-2-3 remained. In these latter experiments there was not a consistent preferred orientation. Instead, it was typically found that only one or two Y1-2-3 crystals nucleated, in random orientations, at the cold end, and normally one of these then developed to form a quasi-single crystal throughout the sample. The observed final orientations ranged from nearly 90° to ca. 10° between the growth axis and the [0 0 1] axis. Selvamanickam *et al.* [25] have argued that the 45° orientation between growth direction and [0 0 1] axis seen in their samples was due to a lateral temperature gradient across the sample. However, this explanation does not appear to be correct for the present set of experiments since a random [0 0 1] orientation developed in the absence of a polycrystalline seed but with an otherwise unaltered experimental configuration.

Instead, the development of a well-defined texture can be explained by the existence of a preferred growth direction in the crystals. For a given imposed rate of isotherm migration (as determined, for example, by the translation rate of the sample) the crystal which will grow directionally at the smallest undercooling below the liquidus temperature will be that which has its preferred growth direction closest to the axis of the rod. Crystals with their preferred growth direction at an angle to the rod axis will be forced to grow faster, i.e. at a larger undercooling, to keep pace with the isotherm migration rate. In a positive temperature gradient they will therefore lag behind the favourably oriented crystals and eventually be overgrown, leading to the preferred texture development.

As well as the preferred growth direction, the three-dimensional shape of the faceted crystal also needs to be considered. The sequential sections in Fig. 8 reveal that the crystal was growing with its faces mutually perpendicular. This is consistent with a recent study by Nakamura *et al.* [26] who showed, from X-ray pole figure analysis, that the growing faces were the (1 0 0), (0 1 0) and (0 0 1) planes. They also determined the growth direction to be perpendicular to the {1 1 2} plane. The {1 1 2} plane is ca. 65° away from (0 0 1), and so this growth direction is somewhat different from that found in the present work and clearly further investigation is required to clarify this.

Finally, an obvious feature of the structure is that a quasi-single crystal was able to develop only because the properitectic particles of the Y2-1-1 phase did not act as efficient heterogeneous nucleation centres for Y1-2-3. This view is supported by previously published transmission electron microscopy results [21, 27] which demonstrated that in samples grown under identical conditions there was no preferred orientation relationship between Y1-2-3 and Y2-1-1. The absence of good nucleation centres is also confirmed by previous experiments which resulted in the growth of large grains in isothermally transformed samples [9]. However, at sufficiently high growth rates and at temperature gradients $< 3.5\,K\,mm^{-1}$, it was possible to form elongated or equiaxed polycrystalline grain structures where nucleation did occur heterogeneously in the bulk of the L plus Y2-1-1. The conditions required for this to occur agree well with the structure selection map originally published by Cima *et al.* [24], but the nucleation centres have not been identified.

4.2. Microstructure development

It has been proposed [23, 25] that continuous growth of the peritectic Y1-2-3 phase is possible because dissolution of the properitectic Y2-1-1 occurs ahead of the advancing solidification front. Fluxes of the species necessary for Y1-2-3 growth are provided by this dissolution process. However, these models do not consider either the mechanism of Y2-1-1 engulfment or the formation of a layered structure with Ba–Cu-rich bands parallel to the (0 0 1) plane. The engulfment process probably follows a sequence first proposed by Hillert [28], shown schematically in Fig. 10. The peritectic solid phase, Y1-2-3, grows along the surface of the properitectic Y2-1-1 with short-range

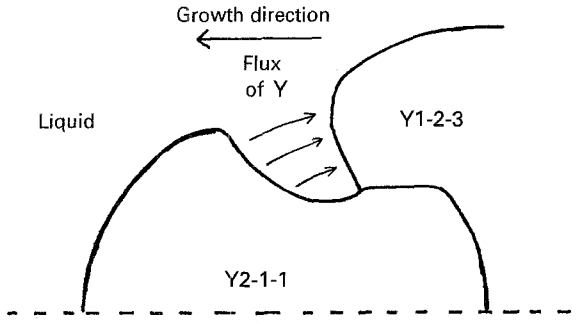

Figure 10 Schematic illustration of the growth of the peritectic Y1-2-3 around the properitectic Y2-1-1 and involving the reaction L + Y2-1-1 → Y1-2-3. (After Ref. 28.)

diffusional fluxes supporting the reaction. It is proposed that the mechanism for the formation of a layered structure is directly related to the engulfment process when growth is in the [0 0 1] direction. Firstly, let us examine the evidence for the effect that Y2-1-1 particles have on the formation of a layered structure. It is well known [13–15] that single crystals produced by flux growth techniques from a melt are often thin in the [0 0 1] direction compared to the [0 1 0] or [1 0 0] directions. On the other hand, crystals prepared by the cooling of (Y2-1-1 + L) exhibit much larger [0 0 1]-axis dimensions, albeit with interconnected layers. The mechanism proposed for formation of layers is depicted schematically in Fig. 11. It is suggested that the local diffusion field around a dissolving Y2-1-1 particle causes a bridge to grow out from the Y1-2-3 in the [0 0 1] axis direction. As the Y1-2-3 grows around the Y2-1-1 it exposes [1 0 0] and [0 1 0] growth directions which are able to spread laterally very rapidly, so causing a macroscopic layer to form with a thickness of the order of a Y2-1-1 particle. Macroscopic steps will first develop where the kinetic undercooling is largest, i.e. at the root of the crystal, as observed in Fig. 9a. The macroscopic steps then advance towards the crystal tip and in so doing trap a thin layer of liquid as they grow, giving rise to the Ba–Cu-rich platelets and the layered crystal structure.

4.3. Sample composition and interface growth temperature

It was observed that the composition of the quenched semi-solid was markedly different from the stoichiometric Y1-2-3 composition of the precursor polycrystalline material. It is believed that two main processes were taking place which contributed to this change. Firstly, the alumina support bars were found to be well wetted by the liquid phase. They were found to be extensively coated by a compound rich in Ba and also containing some Cu. Secondly, liquid was found to have migrated down the temperature gradient and to have penetrated the initially unmelted polycrystalline seed. There were three pieces of evidence for this. Firstly, the seed-end of directionally solidified samples always increased in diameter and gained weight; the gain in weight of the seed was of the order of 30%. Secondly, microstructural analysis revealed the presence of Ba–Cu-rich pools amongst the polycrystalline grains. Thirdly, the average composition of the unmelted seed (as determined by electron probe microanalysis) was found to have become significantly enriched in Ba and marginally in Cu. This phenomenon of liquid migration down a temperature gradient has been noted previously [29] when Y1-2-3 samples were sintered in a steep thermal gradient.

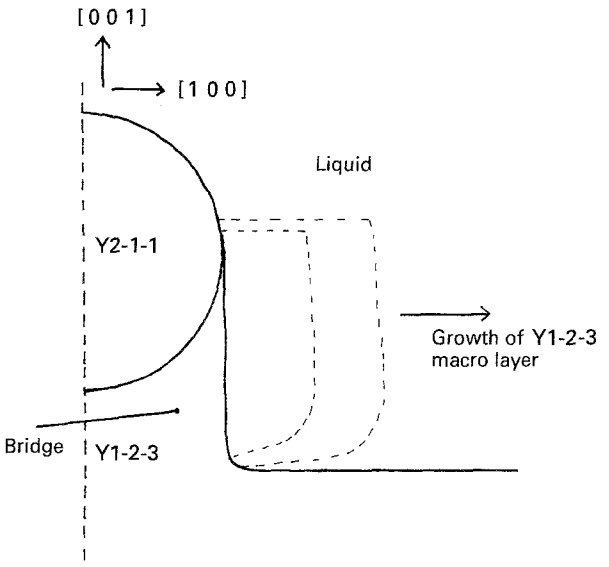

Figure 11 Schematic illustration of the formation of a bridge of Y1-2-3 to a Y2-1-1 particle for growth in the [0 0 1] axis direction. Engulfment of the particle causes [0 1 0] and [1 0 0] directions to be exposed.

The overall loss of liquid and consequential change in composition of the solidifying sample therefore means that the growth undercooling cannot be readily deduced from the measured interface temperature of 940 °C, which is 15–25 K lower than that measured by Cima *et al.* [24] at a similar growth rate. However, the low growth temperature is consistent with an off-stoichiometric composition because the data available on the liquidus surface of the ternary phase diagram [10, 11] indicates a lowering of the peritectic reaction temperature away from stoichiometry. The changing composition of the semi-solid, L + Y2-1-1 region must also have been responsible for the breakdown of quasi-single crystal growth as shown in Fig. 5. Finally, the observation that $BaCuO_2$, with only very small amounts of Y dissolved in it, formed from the quenched liquid is also in accord with the proposed ternary phase diagram relationships [10, 11] for liquid composition.

5. Conclusions

1. Quasi-single crystals of Y1-2-3 can be grown using a technique of horizontal directional solidification in which the sample is supported by 0.5 mm diameter alumina rods. The growth rate required is 1 mm h^{-1} at temperature gradients in the range of 3.5–5 K mm^{-1}.
2. In quasi-single crystals which have been grown from polycrystalline seeds it is found that the [0 0 1] axis is consistently at 45° to the growth axis. No such preferred orientation is observed in samples solidified

without a polycrystalline seed. It is thus concluded that the preferred orientation develops by a competitive growth process from a large number of available orientations.

3. The growth mechanisms can be studied in samples which have been quenched in air to preserve the shape of the solidifying interface. It is found that the macroscopic, solid–liquid facet planes of the Y1-2-3 crystal are mutually perpendicular. Macroscopic steps are seen to develop at the root of the crystal on the (0 0 1) plane. It is proposed that these steps are responsible for the formation of Ba-Cu-rich layers (or bands). Y2-1-1 particles are observed to be engulfed by the Y1-2-3 phase during growth.

4. The loss of liquid from the semi-solid, L plus Y2-1-1 region during crystal growth is found to occur by both substrate wetting and liquid phase migration into the original seed. The changing composition of the remaining liquid is probably responsible for the breakdown of quasi-single crystal growth.

Acknowledgements

The authors are grateful to Dr G.J. Tatlock (University of Liverpool) and Dr P. Regnier (CEA, Saclay, France) for many useful discussions regarding aspects of this work. The assistance of Dr P. Fox and CEA, Saclay, in performing electron probe microanalysis is also acknowledged. X. Yao received financial support from the British Council and much of the work was performed under the BRITE/EURAM contract 0067 CEDB.

References

1. M. MURAKAMI, *Supercond. Sci. Technol.* **5** (1992) 185.
2. P. J. McGINN, W. CHEN and N. ZHU, *J. Metals* **43** (March 1991) 26.
3. S. JIN, T. H. TIEFEL, R. C. SHERWOOD, R. B. VAN DOVER, M. E. DAVIS, G. W. KAMLOTT and R. A. FASTNACHT, *Phys. Rev. B* **37** (1988) 7850.
4. S. JIN, T. H. TIEFEL, R. C. SHERWOOD, M. E. DAVIS, R. B. VAN DOVER, G. W. KAMLOTT, R. A. FASTNACHT and H. D. KEITH, *Appl. Phys. Lett.* **52** (1988) 2074.
5. P. J. McGINN, W. CHEN and M. A. BLACK, *Physica C* **161** (1989) 198.
6. K. SALAMA, V. SELVMANICKAM, L. GAO and K. SUN, *Appl. Phys. Lett.* **54** (1989) 2352.
7. M. MURAKAMI, M. MORITA and N. KOYAMA, *Jpn. J. Appl. Phys.* **28** (1989) L1125.
8. M. MURAKAMI, M. MORITA, K. DOI and M. MIYAMOTO, *ibid.* **28** (1989) 1189.
9. R. J. POLLARD, D. G. McCARTNEY, N. McN. ALFORD and T. BUTTON, *Supercond. Sci. Technol.* **2** (1989) 169.
10. T. ASELAGE and K. KEEFER, *J. Mater. Res.* **3** (1988) 1279.
11. J. SESTAK, *Pure and Appl. Chem.* **64** (1992) 125.
12. H. FREDRIKSSON and T. NYLEN, *Metal Science* **16** (1982) 283.
13. K. N. R. TAYLOR, P. S. COOK, T. PUZZER, D. N. MATTHEWS, G. J. RUSSELL and P. GOODMAN, *J. Cryst. Growth* **88** (1988) 541.
14. K. N. R. TAYLOR, P. S. COOK, D. N. MATTHEWS and P. GOODMAN, *Physica C* **153–155** (1988) 411.
15. TH. WOLF, W. GOLDACKER, B. OBST, G. ROTH and R. FLÜKIGER, *J. Crystal Growth* **96** (1989) 1010.
16. N. McN. ALFORD, T. W. BUTTON, C. E. GOUGH, F. WELLHOFER, D. A. O'CONNOR, M. S. COLCLOUGH, R. J. POLLARD and D. G. McCARTNEY, *J. Appl. Phys.* **66** (1989) 5930.
17. C. AGUILLON, D. G. McCARTNEY, P. REGINIER, S. SENOUSSI and G. J. TATLOCK, *ibid.* **69** (1991) 8261.
18. N. McN. ALFORD, J. D. BIRCHALL, A. J. HOWARD, K. KENDALL, J. H. RAISTRICK, European Patent 183453, 1986.
19. P. FOX, E. J. HARDMAN, J. RINGNALDA, X. YAO, C. J. KIELY, D. G. McCARTNEY and G. J. TATLOCK in Proceedings of the Second European Conference on Advanced Materials and Processes, edited by T. W. Clyne and P. J. Withers (Institute of Materials, London, 1992) Vol. 3, p. 65.
20. A. KELLY and G. W. GROVES, "Crystallography and crystal defects" (Longman, London, 1970) p. 55.
21. J. RINGNALDA, PhD thesis, University of Liverpool, UK (1992).
22. J. RINGNALDA, X. YAO, D. G. McCARTNEY, C. J. KIELY and G. J. TATLOCK, *Mater. Lett.* **13** (1992) 357.
23. T. IZUMI, Y. NAKAMURA and Y. SHIOHARA, *J. Mater. Res.* **7** (1992) 1621.
24. M. J. CIMA, M. C. FLEMINGS, A. M. FIGUEREDO, M. NAKADE, H. ISHII, H. D. BRODY and J. S. HAGGERTY, *J. Appl. Phys.* **72** (1992) 179.
25. V. SELVAMANICKAM, C. PARTISINEVELOS, A. V. McGUIRE and K. SALAMA, *Appl. Phys. Lett.* **60** (1992) 3313.
26. Y. NAKAMURA, K. FURUYA, T. IZUMI and Y. SHIOHARA, *J. Mater. Res.* **9** (1994) 1351.
27. J. RINGNALDA, C. J. KIELY, R. J. POLLARD and D. G. McCARTNEY in Proceedings of the XIIth International Congress for Electron Microscopy, San Francisco, 1990, edited by D. B. Williams (San Francisco Press, San Francisco, 1990) p. 24.
28. M. HILLERT, in "Solidification and casting of metals" (The Metals Society, London, 1979) p. 81.
29. M. N. RAHAMAN, L. C. de JANGHE and M. Y. CHU, *J. Amer. Ceram. Soc.* **71** (1988) C-237.

Received 14 November 1994
and accepted 15 March 1995